Biomass Conversion and Biorefinery (2020) 10:1291–1300
https://doi.org/10.1007/s13399-020-00744-8

ORIGINAL ARTICLE

Removal of levulinic acid from aqueous solutions by clay nano-adsorbents: equilibrium, kinetic, and thermodynamic data

Nilay Baylan[1]

Received: 24 February 2020 / Revised: 10 April 2020 / Accepted: 29 April 2020 / Published online: 11 May 2020

Abstract

In this research, the removal of levulinic acid from aqueous solutions was examined by using clay nano-adsorbents, namely montmorillonite and Cloisite 20A. The batch adsorption experiments were exerted at a different contact time (30–210 min), initial levulinic acid concentrations (20–100 g L^{-1}), adsorbent amounts (0.05–0.25 g), and temperatures (25–45 °C). The equilibrium, kinetic, and thermodynamic data were obtained by using the adsorption capacities of clay nano-adsorbents. It was found that Cloisite 20A exhibited a higher adsorption capacity than montmorillonite. Different adsorption isotherm and kinetic models were utilized to explain the adsorption mechanism and the parameters of these models were determined. Moreover, the thermodynamic analysis was performed to express the adsorption process. For the adsorption of levulinic acid on both clay nano-adsorbents, the adsorption equilibrium data were well represented by the Freundlich isotherm model and the adsorption kinetic data were well characterized by the pseudo-second-order kinetic model for the removal of levulinic acid by two clay nano-adsorbents.

Keywords Levulinic acid · Adsorption · Clay nano-adsorbent · Montmorillonite · Cloisite 20A

1 Introduction

Levulinic acid contains a ketone carbonyl group and an acidic carboxyl group and it is called as keto acid. Levulinic acid is a remarkable versatile acid with a wide range of uses in various areas. It is utilized as a coating material, antifreeze, plasticizer, solvent, stabilizer, food flavoring, and animal feed. Furthermore, it has many uses in the polymer, coating, printing, textile, and pharmaceutical industries as well as in the manufacturing of nylon and rubber, glass-like synthetic fibers and resins, and hydraulic brake fluids [1].

Levulinic acid is mostly produced by the hydrothermal degradation of carbohydrate-containing materials. Firstly, the carbohydrate source is hydrolyzed to form hydroxymethyl furfural in the presence of diluted mineral acid. In the next stage, hydroxymethyl furfural is hydrolyzed and levulinic acid occurs. Furthermore, by-products can form during this process and acid production efficiency decreases with by-product formation. So, the cost and complexity of the acid purification and recovery process increase [1]. Thereby, the by-products require to be removed from the final product. However, levulinic acid can be also produced by fermentation of sucrose that is a biotechnological production method of great importance, and it is obtained in the form of aqueous solutions during the fermentation [2, 3]. The obtained acid should be removed from the water to carry out the fermentation process continuously [4]. The purification step of the manufacturing process is important to decrease the production costs and increase energy efficiency and improve economic performance and environmental impact [5, 6]. Hence, it is substantial to remove and purify levulinic acid during the manufacturing processes as well as from aqueous media or wastewater formed in the use of the chemical industries.

A lot of separation techniques, including extraction, adsorption, ion-exchange, precipitation, ultrafiltration, nanofiltration, electrodialysis, reverse osmosis, membrane separation, and distillation have been extensively employed to remove carboxylic acids from water [7–9]. Among these techniques, extraction [10], nanofiltration and electrodialysis

✉ Nilay Baylan
nilay.baylan@istanbul.edu.tr

[1] Department of Chemical Engineering, İstanbul University-Cerrahpaşa, Avcılar, 34320 İstanbul, Turkey

Table 1 The characteristic properties of clays

Properties	Montmorillonite	Cloisite 20A
Molecule formula	$(Na, Ca)_{0.3}(Al, Mg)_2Si_4O_{10}(OH)_2 \cdot nH_2O$	$(Na, Ca)_{0.3}(Al, Mg, Fe)_2Si_4O_{10}(OH)_2 \cdot nH_2O$
Form	Powder	Powder
Surface modifier	-	Quaternary ammonium
Specific gravity	2.86 g/cm^3	1.77 g/cm^3
Cation exchange capacity	92.6 meq/100 g clay	95 meq/100 g clay
d-spacing (d_{001})	1.17 nm	3.15 nm

[11], and adsorption [12, 13] have been employed to remove levulinic acid from aqueous solutions. Adsorption is an effective process, because it has substantial features, like high separation efficiency, quick response, simplicity, absence of sludge, low instrumentation and operation costs, and applicability of diverse adsorbents [14, 15].

Various adsorbents such as activated carbon [16], Amberlite XAD-4 [12], Amberlite IRA-67 [17], basic polymeric adsorbents (335 resin, D301, D315) [13, 18, 19], and microporous hyper-cross-linked polymers [20, 21] have been investigated in the adsorption of levulinic acid. It is noted that the adsorption studies of levulinic acid were limited. Recently, the usage of nano-adsorbents in adsorption processes has gained importance since they exhibit better adsorption properties [22]. Especially, there is a growing demand for testing nano-adsorbents in the removal of organic compounds from aqueous solutions. Clays are natural, environmentally friendly substances with a high specific surface area and are extensively preferred for the adsorption and removal of various substances [23, 24]. Besides, they have a low-cost compared with conventional adsorbents. The most commonly used clay as nano-adsorbent is montmorillonite. Montmorillonite is a kind of clay material that is abundant in nature [25]. Nano-adsorbent Cloisite 20A clay is montmorillonite modified by adding quaternary ammonium salts. Based on these properties of clays, in this study, montmorillonite and Cloisite 20A clays are considered as novel adsorbents for the uptake of levulinic acid from aqueous solutions because montmorillonite and Cloisite 20A (modified montmorillonite) as clay nano-adsorbents have not been examined in levulinic acid adsorption so far. Hence, in this adsorption research, clay nano-adsorbents were tested and compared for the adsorption of levulinic acid. For this purpose, the effects of various adsorption factors like contact time, initial acid concentration, adsorbent amount, and temperature were investigated. So, the equilibrium, kinetic, and thermodynamic data were obtained to characterize the adsorption process.

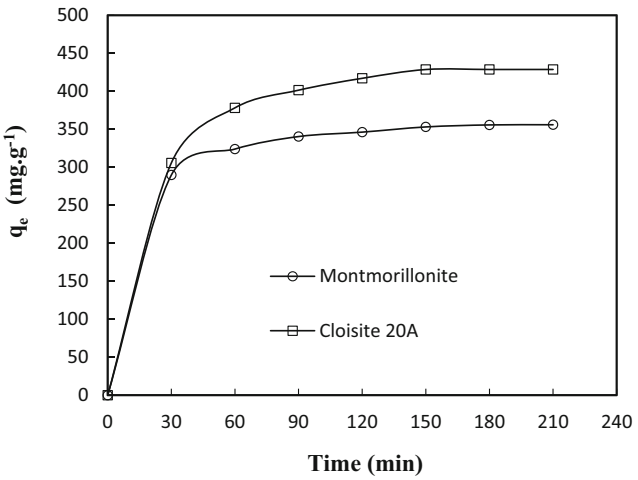

Fig. 1 The variation of levulinic acid adsorption over time for montmorillonite and Cloisite 20A. Operating conditions: C_0 = 100 g L^{-1}, M = 0.05 g, and T = 25 °C

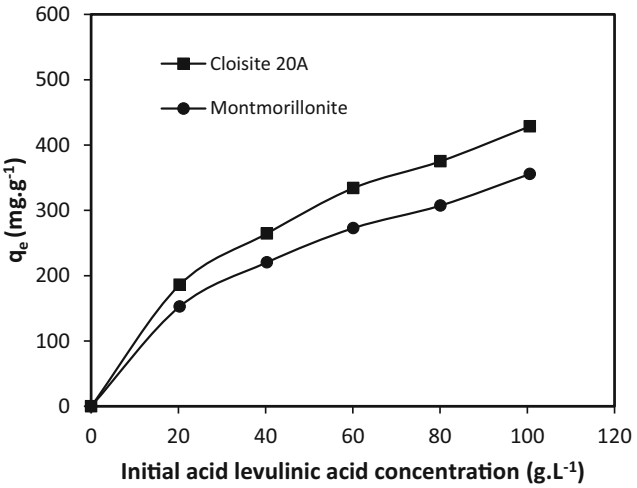

Fig. 2 The effect of initial acid concentration on levulinic acid adsorption by montmorillonite and Cloisite 20A. Operating conditions: M = 0.05 g, T = 25 °C, and t = 180 min

2 Materials and method

Aqueous acid solutions with different concentrations were prepared by dissolution of levulinic acid (> 98%) in distilled water. Levulinic acid was supplied from ACROS Organics. Montmorillonite (98%) and Cloisite 20A (> 97%) were obtained from Southern Clay Products (Texas, U.S.A.). Montmorillonite is a hydrated aluminum silicate with sodium as the dominant cation exchanger. Cloisite 20A is montmorillonite modified by adding dimethyl dihydrogenated tallow quaternary ammonium chloride. Tallow is derived from beef and is mainly consists of 18 carbon chains (approximately 65% C18, 30% C16, and 5% C14). Hydrogenated tallow is obtained from tallow by the hydrogenation of double bonds. Cloisite 20A consists of 2 tallow groups; hence, it is more hydrophobic [26]. The clays were used without further treatment. The main characteristic properties of clays provided by the supplier were also summarized in Table 1. The operating ranges of adsorption parameters such as initial acid concentration, adsorbent amounts, and temperature were determined from the preliminary experiments. So, batch adsorption experiments were exerted by shaking glass Erlenmeyer flasks containing 5 mL levulinic acid solutions (concentrations of 20–100 g L^{-1}) and adsorbents (amounts of 0.05–0.25 g) in a water bath for the determined equilibrium time (180 min) at different temperatures (25–45 °C). The rate of shaker (Nüve ST 30) was 150 rpm. After adsorption operation, the samples were filtered and the adsorbents were separated from the aqueous solutions by utilizing the filtration procedure. The levulinic acid concentrations before and after the adsorption operation were detected by using SI Analytics automatic titrator using 0.1 N NaOH.

Adsorption capacity (q_e, mg g^{-1}) of adsorbents at equilibrium for levulinic acid adsorption were calculated from the following Eq. (1):

$$q_e = \left[\frac{(C_0 - C_e)}{M}\right] * V \quad (1)$$

where C_0 signifies the initial acid concentration (mg L^{-1}); C_e denotes the equilibrium acid concentration (mg L^{-1}); V represents the volume of solution (L); and M symbolizes the quantity of adsorbents (g).

3 Results and discussion

3.1 Determination of equilibrium adsorption time

To determine the equilibrium time, the batch experiments were exerted using an initial concentration of levulinic acid solution of 100 g L^{-1} and a clay amount of 0.05 g. Figure 1 shows the variation of levulinic acid adsorption over time for both adsorbents. As can be observed from Fig. 1, the levulinic acid adsorption increased as time increased in the initial stages; then, the adsorption slowed until equilibrium was attained because, initially, adsorption is quick owing to the free adsorption zones on the adsorbent surface. The adsorption then slows down because of the reduction in the number of adsorption sites present. Considering the values of the adsorption capacity of both adsorbents depicted in Fig. 1, it was seen

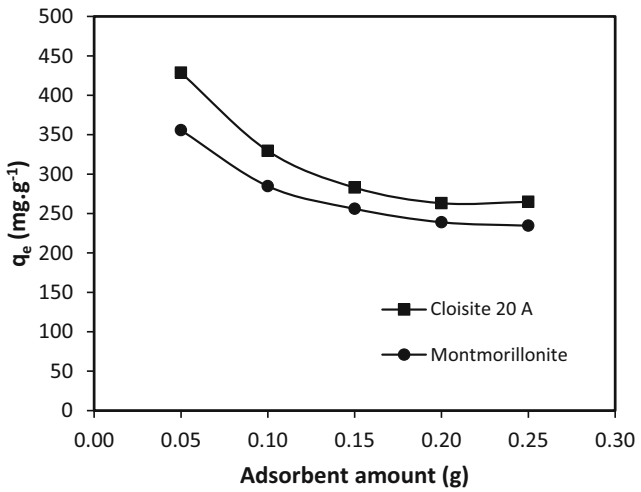

Fig. 3 The effect of amounts of montmorillonite and Cloisite 20A on levulinic acid adsorption. Operating conditions: C_0 = 100 g L^{-1}, T = 25 °C, and t = 180 min

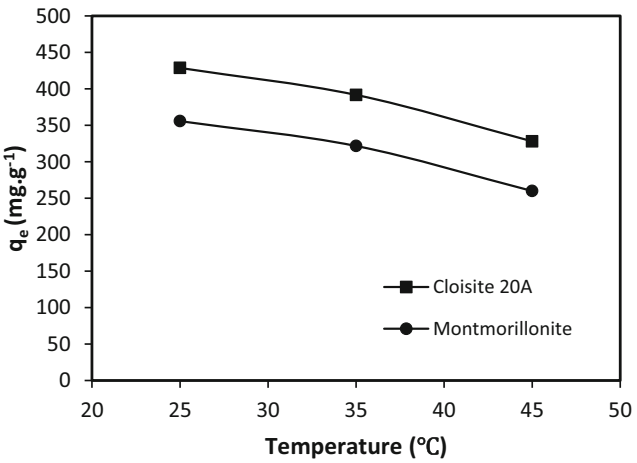

Fig. 4 The effect of temperature on levulinic acid adsorption by montmorillonite and Cloisite 20A. Operating conditions: C_0 = 100 g L^{-1}, M = 0.05 g, and t = 180 min

Table 2 Adsorption isotherm models

Isotherm models	Equations	
Langmuir isotherm model	Non−linear form : $q_e = \frac{Q_m K_L C_e}{1+K_L C_e}$	(2)
	Linear form : $\frac{1}{q_e} = \frac{1}{Q_m} + \left(\frac{1}{K_L * Q_m}\right) * \left(\frac{1}{C_e}\right)$	(3)
	Plot : $\frac{1}{q_e}$ vs. $\frac{1}{C_e}$	
	K_L: Langmuir isotherm constant (L mg^{-1}) Q_m: maximum adsorption capacity (mg g^{-1})	
Freundlich isotherm model	Non−linear form : $q_e = K_f C_e^{\frac{1}{n}}$	(4)
	Linear form : $\log q_e = \log K_f + \frac{1}{n}\log C_e$	(5)
	Plot : $\log q_e$ vs. $\log C_e$	
	K_f:Freundlich isotherm constant related to adsorption capacity (mg g^{-1}) (L mg^{-1})^n n: Freundlich isotherm constant related to adsorption intensity	
Temkin isotherm model	Non−linear form : $q_e = B\ln(K_t C_e)$; $B = \frac{RT}{b_t}$	(6)
	Linear form : $q_e = \mathrm{B}\ \mathrm{In}K_t + B \ln C_e$	(7)
	Plot : q_e vs. $\ln C_e$	
	K_t: Temkin isotherm constant (L g^{-1}) b_t: Temkin isotherm constant related to adsorption heat (J mol^{-1})	

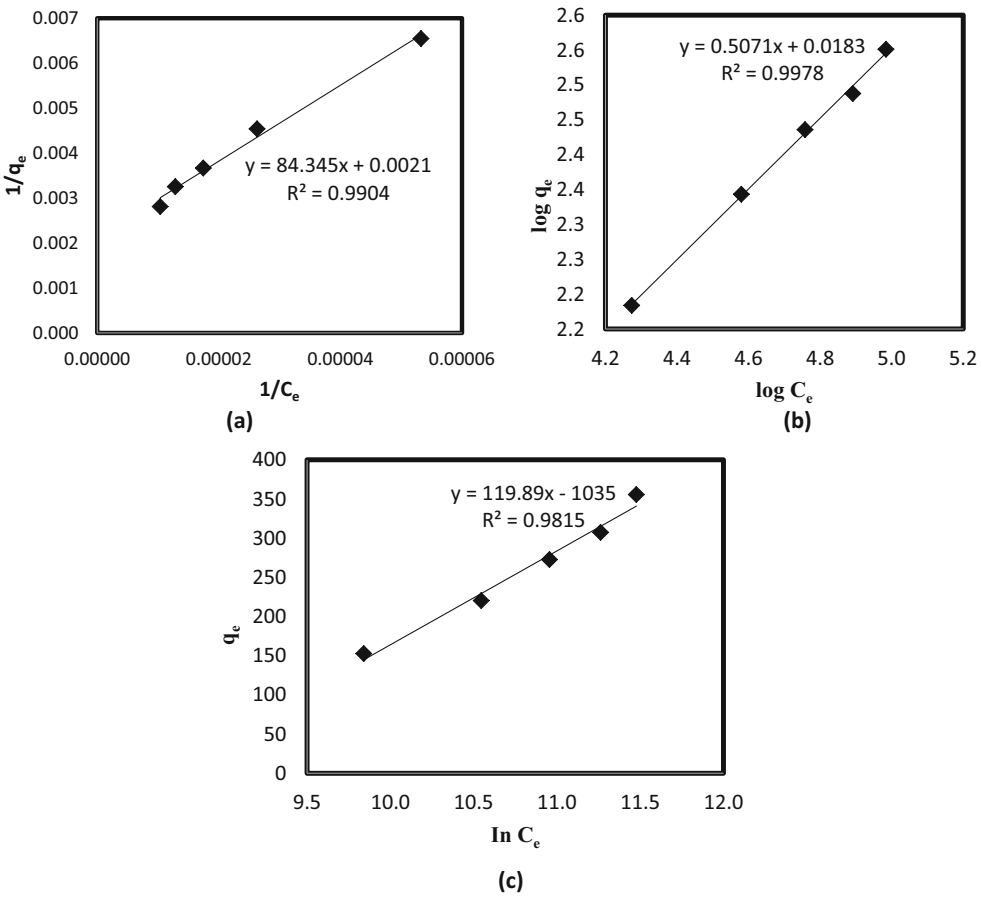

Fig. 5 Linear fits of **a** Langmuir, **b** Freundlich, and **c** Temkin isotherm models for the levulinic acid adsorption by montmorillonite

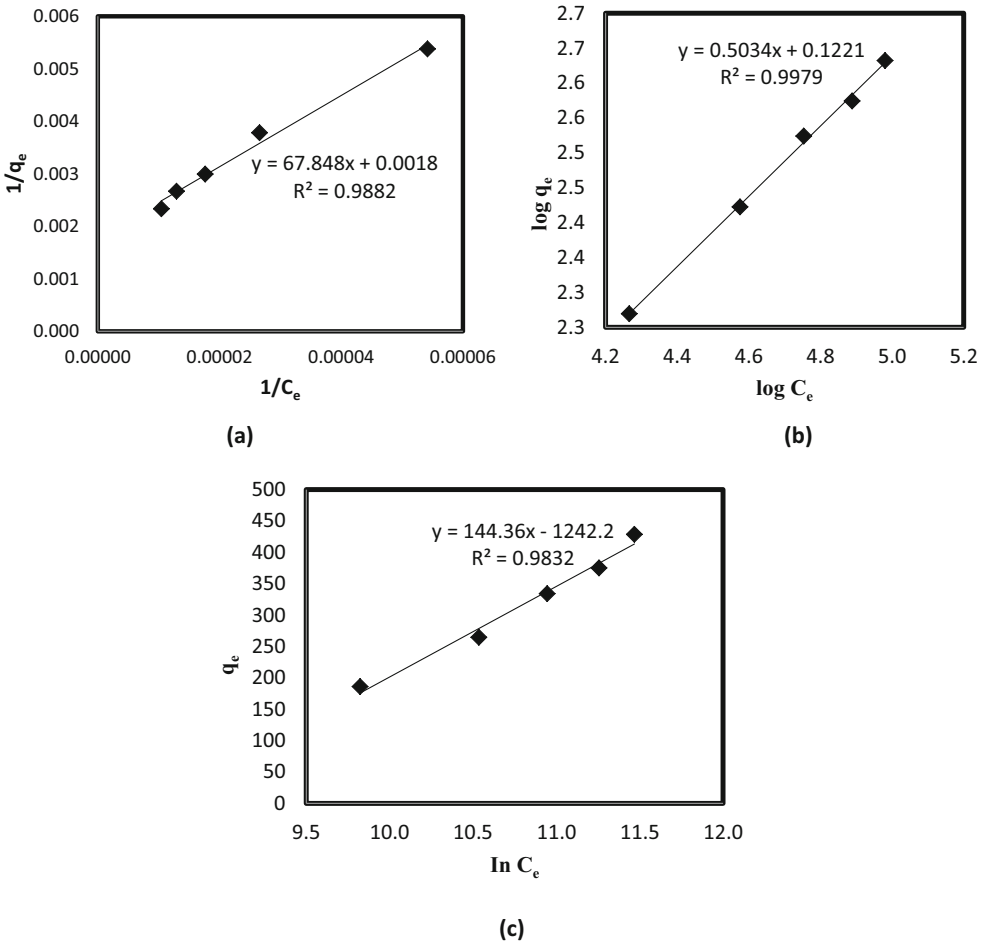

Fig. 6 Linear fits of **a** Langmuir, **b** Freundlich, and **c** Temkin isotherm models for the levulinic acid adsorption by Cloisite 20A

that the adsorption had reached the equilibrium between 150 and 180 min. So, the equilibrium adsorption time was determined as 180 min.

3.2 The effect of initial acid concentration

In order to examine the effect of initial acid concentration on adsorption, the experiments were exerted using five concentrations of levulinic acid of about 20, 40, 60, 80, and 100 g L^{-1} with the period of equilibrium adsorption time at 25 °C. The adsorbent amount utilized was 0.05 g. The results of these experiments were plotted in Fig. 2. When Fig. 2 was examined, it can be seen that the values of adsorption capacity increased from 152.70 to 355.69 mg g^{-1} for montmorillonite and from 185.99 to 428.63 mg g^{-1} for Cloisite 20A with the increasing the levulinic acid concentration. Uslu et al. [17] separated levulinic acid from its aqueous solutions by Amberlite IRA-67 and they also found that the adsorption capacity increased with the increased concentration of acid. Similarly, Datta and Uslu [12] investigated the levulinic acid adsorption with Amberlite XAD-4. They reported that the values of adsorption capacity increased with an increase in the initial concentration of levulinic acid in the solution.

Table 3 Isotherm parameters and regression coefficients for levulinic acid adsorption by montmorillonite and Cloisite 20A

Adsorbents	Isotherm parameters and regression coefficients									
	Langmuir			Freundlich			Temkin			
	Q_m (mg g^{-1})	K_L (L mg^{-1})	R^2	K_f (mg g^{-1}) (L $mg^{-1})^n$	n	R^2	K_t (L g^{-1})	B	b_t (J mol^{-1})	R^2
Montmorillonite	476.190	$2.5.10^{-5}$	0.9904	1.043	1.972	0.9978	$1.79.10^{-4}$	119.89	20.665	0.9815
Cloisite 20A	555.556	$2.7.10^{-5}$	0.9882	1.325	1.986	0.9979	$1.84.10^{-4}$	144.36	17.162	0.9832

Table 4 Adsorption kinetic models and equations

Kinetic models	Equations	
Pseudo-first-order model	Non−linear form : $\frac{dq_t}{dt} = k_1 * (q_e - q_t)$	(8)
	Linear form : $\ln(q_e - q_t) = \ln q_e - k_1 t$	(9)
	Plot : $\ln(q_e - q_t)$ vs. t	
	k_1: pseudo-first-order kinetic rate coefficient (min^{-1})	
Pseudo-second-order model	Non−linear form : $\frac{dq_t}{dt} = k_2 * (q_e - q_t)^2$	(10)
	Linear form : $\frac{t}{q_t} = \frac{1}{k_2 * q_e^2} + \frac{1}{q_e} * t$	(11)
	Plot : $\frac{t}{q_t}$ vs. t	
	k_2: pseudo-second-order kinetic rate coefficient (g mg^{-1} min^{-1})	
Elovich model	Non−linear form : $\frac{dq}{dt} = \alpha * \exp(-\beta * q_t)$	(12)
	Linear form : $q_t = \frac{1}{\beta} * \ln(\alpha * \beta) + \frac{1}{\beta} * \ln t$	(13)
	Plot : q_t vs. $\ln t$	
	α: initial adsorption rate (mg g^{-1} min^{-1})	
	β: the constant of desorption (g mg^{-1})	

Notes: q_e, the adsorption capacity of the adsorbent at the equilibrium (mg g^{-1}); q_t, the adsorption capacity of the adsorbent at the time (t) (mg g^{-1})

3.3 Effect of adsorbent amount

The effect of the adsorbent amount was examined by using various amounts varied between 0.05 and 0.25 g at the initial acid concentration of 100 g L^{-1} at 25 °C. The effect of adsorbent amount on the adsorption capacity for levulinic acid was depicted in Fig. 3. It was seen from Fig. 3 that the values of adsorption capacity decreased with the increase in the amount of nano-adsorbents. The maximum adsorption capacity values were obtained as 428.63 mg g^{-1} for Cloisite 20A and

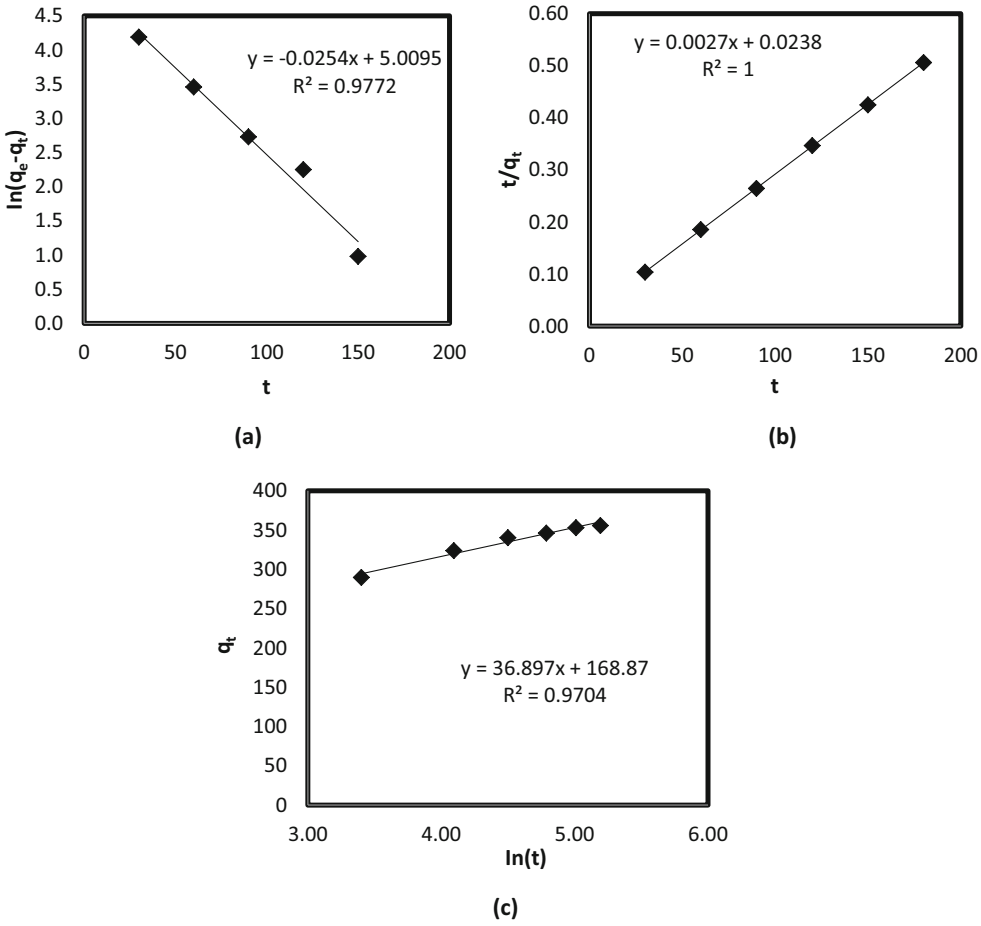

Fig. 7 Linear fits of **a** pseudo-first-order, **b** pseudo-second-order, and **c** Elovich kinetic models for levulinic acid adsorption by montmorillonite

355.69 mg g^{-1} for montmorillonite in case of using an amount of 0.05 g.

3.4 Effect of temperature

To observe the effect of temperature on levulinic acid adsorption by montmorillonite and Cloisite 20A, the experiments were exerted at three dissimilar temperatures (25, 35, and 45 °C). The initial levulinic acid concentration of about 100 g L^{-1} and the adsorbent amount of 0.05 g were used. The acquired results were demonstrated in Fig. 4. As can be seen from Fig. 4, the values of adsorption capacity were decreased with an increase in temperature, and the trends were obtained as same for both adsorbents. It was clear from these results that the adsorption of levulinic acid by montmorillonite and Cloisite 20A was exothermic. This result was confirmed by observations from similar studies of levulinic acid [12, 17].

3.5 Equilibrium adsorption models

The equilibrium data were appraised by utilizing the adsorption isotherm models including Langmuir, Freundlich, and Temkin isotherm models. The isotherm models and equations were given in Table 2 [27, 28].

Figures 5 and 6 show the linear plots of Langmuir, Freundlich, and Temkin isotherm models for levulinic acid adsorption by montmorillonite and Cloisite 20A, respectively. Table 3 indicates Langmuir, Freundlich, and Temkin isotherm model parameters and regression coefficients calculated from these illustrated linear plots. When the values of regression coefficients given in Table 3 were examined, the Freundlich isotherm model exhibited the best fit to the equilibrium adsorption data of both adsorbents. The Freundlich isotherm model approach assumes that the adsorption occurs multilayer on the adsorbent surface and implies that the adsorbent surface is heterogeneous [22].

3.6 Adsorption kinetic models

The adsorption kinetic of levulinic acid by montmorillonite and Cloisite 20A were examined by utilizing three kinetic models including pseudo-first-order, pseudo-second-order, and Elovich kinetic models. The kinetic models and equations were given in Table 4 [29, 30]. The kinetic experiments were actualized at different contact time intervals (30–180 min) with initial levulinic acid concentration of 100 g L^{-1}, nano-clay amount of 0.05 g, and temperature of 25 °C.

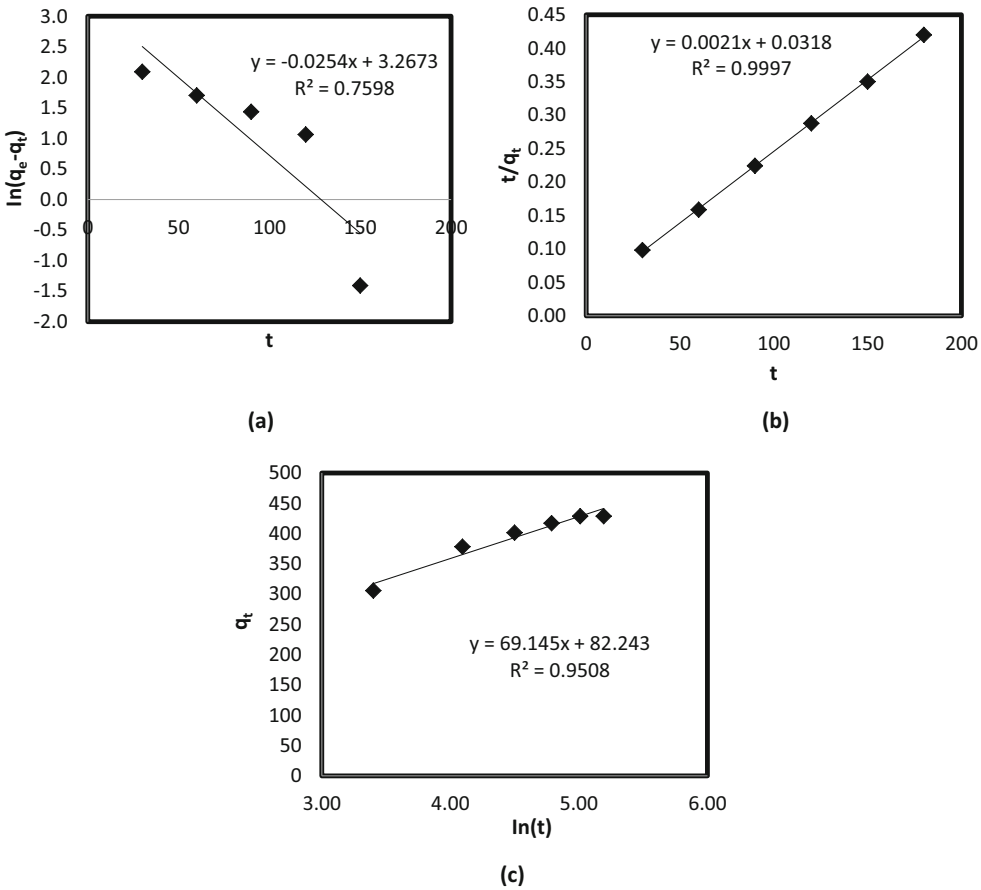

Fig. 8 Linear fits of **a** pseudo-first-order, **b** pseudo-second-order, and **c** Elovich kinetic models for levulinic acid adsorption by Cloisite 20A

Table 5 Kinetic model parameters and regression coefficients for levulinic acid adsorption by montmorillonite and Cloisite 20A

Adsorbents	Kinetic model parameters and regression coefficients								
	Pseudo-first order			Pseudo-second order			Elovich		
	k_1 (min^{-1})	q_e (mg g^{-1})	R^2	k_2 (g mg^{-1} min^{-1})	q_e (mg g^{-1})	R^2	α	β	R^2
Montmorillonite	0.0254	149.75	0.9772	$3.06.10^{-4}$	370.37	1.0000	3585.84	0.0271	0.9704
Cloisite 20A	0.0254	26.24	0.7598	$1.39.10^{-4}$	476.19	0.9997	226.44	0.0145	0.9508

Figures 7 and 8 demonstrate the linear plots of pseudo-first-order, pseudo-second-order, and Elovich kinetic models for levulinic acid adsorption by montmorillonite and Cloisite 20A, respectively. Table 5 shows the kinetic model parameters and regression coefficients calculated from these depicted linear plots. When the values of the regression coefficient shown in Table 5 were analyzed, the pseudo-second-order kinetic model exhibited the best fit to the kinetic adsorption data for both adsorbents. Pseudo-second-order kinetic model implies that the adsorption mechanism depends on the adsorbent and adsorbate [31, 32].

3.7 Adsorption thermodynamic

To investigate levulinic acid adsorption thermodynamic, three different temperatures (25, 35, and 45 °C) were studied at the initial levulinic acid concentration of 100 g L^{-1} and adsorbent amount of 0.05 g. The thermodynamic parameters including Gibb's free energy (ΔG^0), enthalpy (ΔH^0), and entropy (ΔS^0) were determined. ΔG^0, ΔH^0, and ΔS^0 were calculated by means of equations given in Table 6 [33, 34].

Figure 9 shows the linear plots of $\ln(K_D)$ vs. $\frac{1}{T}$ for levulinic acid adsorption by montmorillonite and Cloisite 20A. Table 7 shows thermodynamic parameters (ΔS^0 and ΔH^0) calculated from the intercept and slope of linear plots. As can be seen from Table 7, the adsorption of levulinic acid was exothermic ($\Delta H^0 < 0$) for both nano-adsorbents. It was also found $\Delta S^0 < 0$ indicating that there was a decreased randomness at the adsorbent-adsorbate interface during the adsorption process [34]. In addition, the values of ΔG^0 based on different temperatures were obtained as shown in Table 8. $\Delta G^0 < 0$ implies that adsorption is spontaneous and favorable

Table 6 Adsorption thermodynamic equations

Equations	
Gibb's free energy : $\Delta G^0 = -R*T*\ln(K_D) = -R*T*\ln\left(\frac{q_e}{C_e}\right)$	(14)
Van't Hoff equation : $\ln(K_D) = \frac{-\Delta G^0}{R*T} = \frac{-\Delta H^0}{R*T} + \frac{\Delta S^0}{R}$	(15)
Plot : $\ln(K_D)$ vs. $\frac{1}{T}$	

Notes: ΔG^0, Gibb's free energy (J mol^{-1}); T, temperature (K); R, the gas constant (8.314 J mol^{-1} K^{-1}); ΔH^0, enthalpy (J mol^{-1}); ΔS^0, entropy (J mol^{-1} K^{-1})

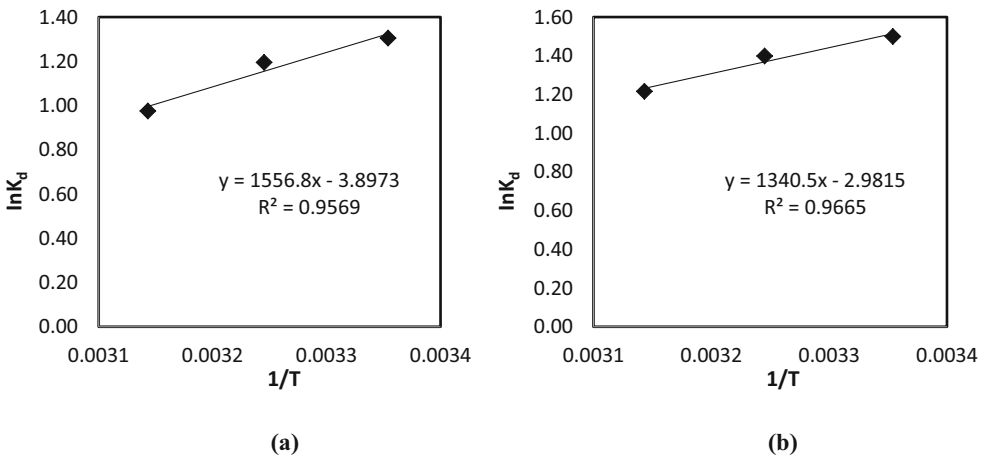

Fig. 9 Linear plots of $\ln(K_D)$ vs. $\frac{1}{T}$ for levulinic acid adsorption by **a** montmorillonite and **b** Cloisite 20A

Table 7 Thermodynamic parameters and regression coefficients for levulinic acid adsorption by montmorillonite and Cloisite 20A

Adsorbents	Thermodynamic parameters and regression coefficients		
	ΔH^0 (J mol^{-1})	ΔS^0 (J mol^{-1} K^{-1})	R^2
Montmorillonite	− 12943	− 32.40	0.9569
Cloisite 20A	− 11145	− 24.79	0.9665

[34]. Thus, the adsorption of levulinic acid by montmorillonite and Cloisite 20A occurs spontaneously and it is favorable (Cloisite 20A > montmorillonite).

3.8 Comparison of adsorption capacities

The abovementioned studies indicated that Cloisite 20A (modified montmorillonite) exhibited a higher selectivity and adsorption capacity than montmorillonite. The difference in the adsorption performance of absorbents can be attributed to the differences in the surface features of the adsorbents. This conclusion has proved that a surface modifier has a significant impact on the adsorption capacity. The modified montmorillonite surface is preferred due to the presence of quaternary ammonium chloride (cationic compound containing alkyl groups in long carbon chains) compared with the unmodified montmorillonite surface and also modified montmorillonite is more hydrophobic [33]. A clay mineral predominantly performs the adsorption with a cation exchange mechanism. The cations can be bonded with electrostatic forces into the surface of adsorbents [15]. In this context, the adsorption phenomenon of levulinic acid onto clays may be explained by the cation exchange mechanism. Table 9 demonstrates a comparison of the adsorption capacity of nano-adsorbents in the present study with the values of the adsorption capacity of various adsorbents reported in the literature for levulinic acid. As shown in Table 9, the adsorption capacity value obtained in this study was quite high compared with other reported capacity values. These results confirmed that montmorillonite and Cloisite 20A are efficient nano-adsorbents for the removal of levulinic acid from aqueous solutions.

Table 8 Gibb's free energy (ΔG^0) for levulinic acid adsorption by montmorillonite and Cloisite 20A

T (°C)	ΔG^0 (J mol^{-1})	
	Montmorillonite	Cloisite 20A
25	− 3235	− 3718
35	− 3062	− 3584
45	− 2580	− 3217

4 Conclusion

The levulinic acid adsorption was tested by utilizing montmorillonite and Cloisite 20A (modified montmorillonite). It was found that these clay nano-adsorbents were effective for the removal of levulinic acid from aqueous solutions. It was also obtained that nano-clay Cloisite 20A exhibited a higher selectivity and adsorption capacity than montmorillonite. The equilibrium, kinetic, and thermodynamic studies were carried out for both adsorbents by investigating the effect of time, acid concentration, and temperature on the adsorption process. The adsorption capacities of adsorbents were increased as the initial levulinic acid concentration increased. The maximum adsorption capacities obtained 428.63 mg g^{-1} for Cloisite 20A and 355.69 mg g^{-1} for montmorillonite. The optimal adsorption operating conditions were determined as the contact adsorption time of 180 min, initial levulinic acid concentration of 100 g L^{-1}, the amount of adsorbent of 0.05 g, and the temperature of 25 °C. The equilibrium data for two adsorbents were best described by the Freundlich isotherm model, demonstrating the multilayer adsorption process. The kinetic data showed a good fit by the pseudo-second-order kinetic model for two adsorbents. From the thermodynamic analysis, the adsorption of levulinic acid on the clay nano-adsorbents was found to be exothermic process. This study indicated that these clay nano-adsorbents are effective and can be used in the removal of levulinic acid from aqueous solutions. Besides, this study has suggested that these adsorbents can be used for the removal of other organic acids from the fermentation broths or mixture or waste solutions.

Table 9 Adsorption capacity values of various adsorbents in the literature for levulinic acid

Adsorbent	Adsorption capacity (q_e, mg g^{-1})	References
Amberlite XAD-4	35.98	[12]
Amberlite IRA-67	47.65	[17]
SY-01 resin	103.74	[20]
MWCNT*	483.25	[35]
Montmorillonite	355.69	This study
Cloisite 20A	428.63	This study

**MWCNT*, multiwall carbon nanotube

References

1. Baylan N, Çehreli S (2018) Ionic liquids as bulk liquid membranes on levulinic acid removal: a design study. J Mol Liq 266:299–308
2. Caballero B, Trugo LC, Finglas PM (2003) Encyclopedia of food sciences and nutrition. Academic .
3. Guad R, Surana S, Talele G, Talele MS, Gokhale MS (2006) Natural excipients. Pragati Books Pvt. Ltd.
4. Kumar S, Babu B (2008) Process intensification for separation of carboxylic acids from fermentation broths using reactive extraction. J Fut Eng Technol 3:19–26
5. Datta D, Marti ME, Pal D, Kumar S (2017) Equilibrium study on the extraction of levulinic acid from aqueous solution with Aliquat 336 dissolved in different diluents: Ssolvent's polarity effect and column design. J Chem Eng Data 62:3–10
6. Long NVD, Lee M (2016) Design and optimization of the levulinic acid recovery process from lignocellulosic biomass. Chem Eng Res Des 107:126–136
7. İnci I, Aydın A (2003) Extraction of hydroxycarboxylic acids with MIBK/Toluene solutions of amines. J Sci Ind Res 62(9):926–930
8. Aşçı YS, Dramur U, Bilgin M (2017) Investigation of the separation of carboxylic acids from aqueous solutions using a pilot scale membrane unit. J Mol Liq 248:391–398
9. Lalikoğlu M, Gök A, Gök MK, Aşçı YS (2015) Investigation of lactic acid separation by layered double hydroxide: equilibrium, kinetics, and thermodynamics. J Chem Eng Data 60:3159–3165
10. Brouwer T, Blahusiak M, Babic K, Schuur B (2017) Reactive extraction and recovery of levulinic acid, formic acid and furfural from aqueous solutions containing sulphuric acid. Sep Purif Technol 185:186–195
11. Kim JH, Na J-G, Yang J-W, Chang YK (2013) Separation of galactose, 5-hydroxymethylfurfural and levulinic acid in acid hydrolysate of agarose by nanofiltration and electrodialysis. Bioresour Technol 140:64–72
12. Datta D, Uslu H (2017) Adsorption of levulinic acid from aqueous solution by Amberlite XAD-4. J Mol Liq 234:330–334
13. Liu B-J, Hu Z-J, Ren Q-L (2009) Single-component and competitive adsorption of levulinic/formic acids on basic polymeric adsorbents. Colloids Surf A Physicochem Eng Asp 339:185–191
14. Awual MR, Eldesoky GE, Yaita T, Naushad M, Shiwaku H, AlOthman ZA, Suzuki S (2015) Schiff based ligand containing nano-composite adsorbent for optical copper (II) ions removal from aqueous solutions. Chem Eng J 279:639–647
15. Baylan N, Meriçboyu AE (2016) Adsorption of lead and copper on bentonite and grapeseed activated carbon in single-and binary-ion systems. Sep Sci Technol 51:2360–2368
16. Liu BJ, Liu SW, Liu TB, Mao JW (2012) Advanced Materials Research. Trans Tech Publ 1691–1695
17. Uslu H, Datta D, Santos D, Öztürk M (2019) Separation of levulinic acid using polymeric resin, Amberlite IRA-67. J Chem Eng Data 64:3044–3049
18. Liu B-J, Ren Q-L (2006) Sorption of levulinic acid onto weakly basic anion exchangers: equilibrium and kinetic studies. J Colloid Interface Sci 294:281–287
19. Liu B, Liu S (2011) Adsorption of levulinic acid from aqueous solution onto basic polymeric adsorbent: experimental and modeling studies. Sep Sci Technol 46:2391–2399
20. Lin X, Huang Q, Qi G, Xiong L, Huang C, Chen X, Li H, Chen X (2017) Adsorption behavior of levulinic acid onto microporous hyper-cross-linked polymers in aqueous solution: equilibrium, thermodynamic, kinetic simulation and fixed-bed column studies. Chemosphere 171:231–239
21. Lin X, Huang Q, Qi G, Shi S, Xiong L, Huang C, Chen X, Li H, Chen X (2017) Estimation of fixed-bed column parameters and mathematical modeling of breakthrough behaviors for adsorption of levulinic acid from aqueous solution using SY-01 resin. Sep Purif Technol 174:222–231
22. Bhatia D, Datta D, Joshi A, Gupta S, Gote Y (2019) Adsorption of isonicotinic acid from aqueous solution using multi-walled carbon nanotubes/Fe_3O_4. J Mol Liq 276:163–169
23. Kyzas GZ, Matis KA (2015) Nanoadsorbents for pollutants removal: a review. J Mol Liq 203:159–168
24. Liu P, Zhang L (2007) Adsorption of dyes from aqueous solutions or suspensions with clay nano-adsorbents. Sep Purif Technol 58: 32–39
25. Hassani A, Kiranşan M, Soltani RDC, Khataee A, Karaca S (2015) Optimization of the adsorption of a textile dye onto nanoclay using a central composite design. Turk J Chem 39:734–749
26. Kumar P, Sandeep K, Alavi S, Truong V, Gorga R (2010) Effect of type and content of modified montmorillonite on the structure and properties of bio-nanocomposite films based on soy protein isolate and montmorillonite. J Food Sci 75:N46–N56
27. Mahmoodi NM, Hayati B, Arami M, Lan C (2011) Adsorption of textile dyes on pine cone from colored wastewater: kinetic, equilibrium and thermodynamic studies. Desalination 268:117–125
28. Yusan S, Gok C, Erenturk S, Aytas S (2012) Adsorptive removal of thorium (IV) using calcined and flux calcined diatomite from Turkey: evaluation of equilibrium, kinetic and thermodynamic data. Appl Clay Sci 67:106–116
29. Yang X, Al-Duri B (2005) Kinetic modeling of liquid-phase adsorption of reactive dyes on activated carbon. J Colloid Interface Sci 287:25–34
30. Yeddou N, Bensmaili A (2005) Kinetic models for the sorption of dye from aqueous solution by clay-wood sawdust mixture. Desalination 185:499–508
31. Meroufel B, Benali O, Benyahia M, Benmoussa Y, Zenasni M (2013) Adsorptive removal of anionic dye from aqueous solutions by Algerian kaolin: characteristics, isotherm, kinetic and thermodynamic studies. J Mater Environ Sci 4:482–491
32. Pavan FA, Dias SL, Lima EC, Benvenutti EV (2008) Removal of Congo red from aqueous solution by anilinepropylsilica xerogel. Dyes Pigments 76:64–69
33. Freitas A, Mendes M, Coelho G (2007) Thermodynamic study of fatty acids adsorption on different adsorbents. J Chem Thermodyn 39:1027–1037
34. Pradhan N, Rene E, Lens P, Dipasquale L, D'Ippolito G, Fontana A, Panico A, Esposito G (2017) Adsorption behaviour of lactic acid on granular activated carbon and anionic resins: thermodynamics, isotherms and kinetic studies. Energies 10:665
35. Çelebican Ö, İnci İ, Baylan N (2020) Investigation of adsorption properties of levulinic acid by a nanotechnological material. J Mol Struct 1203:127454